Available online at www.sciencedirect.com
ScienceDirect
Coastal Engineering 54 (2007) 417–431
Coastal Engineering
An International Journal for Coastal, Harbour and Offshore Engineers
www.elsevier.com/locate/coastaleng

Linear evolution of a shoreface nourishment

S. Van Leeuwen [a,1], N. Dodd [a,*], D. Calvete [b], A. Falqués [b]

[a] School of Civil Engineering, University of Nottingham, University, Park, Nottingham, NG7 2RD, UK
[b] Applied Physics Dept., Universitat Politécnica de Catalunya, Barcelona, Spain

Received 6 March 2006; received in revised form 27 October 2006; accepted 13 November 2006
Available online 19 January 2007

Abstract

The morphological evolution of a shoreface nourishment is investigated by interpreting the nourishment as a linear perturbation of the natural system. The nourishment is projected onto the subset of linear eigenmodes with negative growth rates of the morphodynamical system. The evolution of these linear modes then determines the temporal behaviour of the shoreface nourishment. The method is presented, and results are shown for shoreface nourishments of different length scales on a straight coast and subject to normal incidence. Shoreface nourishments are represented by their expansions according to the projection method on a 1:50 plane beach profile. All nourishments are shown primarily to be diffusive features, with long scale nourishments diffusing more slowly than shorter length scale nourishments. Long scale nourishments also exhibit a shoreward movement during their decay. This all indicates that long length scale nourishments may be more beneficial in coastal engineering projects. This study is a first step towards nonlinear projection to study shoreface nourishment behaviour.

Keywords: Shoreface nourishment; Stability analysis; Morphodynamics

1. Introduction

Coastal areas are often characterised by dense populations and large economic interests, and a healthy beach constitutes the first line of coastal defence. Beaches also represent a vital economic (recreational) asset. Consequently, shore nourishments have become an increasingly popular option for beach preservation.

Different types of shore nourishments exist, depending on where the sediment is placed. This can be on the first dune row, at the duneface, on the beach, in the surf zone or at the shoreface (Hamm et al., 2002). Of these types of nourishments, shoreface nourishments have the advantage of reduced cost: natural forces are assumed to redistribute the sediment shoreward, so that there is no need to scrape the beach. The use of the beach is also not hindered while the nourishment is placed and there is no need to put sediment (generally mined offshore) directly on land. Any reduction in costs is desirable as shoreface nourishments, like all shore nourishments, are expensive, and in general are an ongoing commitment, incurring monitoring expenses as well as those of repeated nourishment.

Because of these perceived advantages shoreface nourishment, in Europe at least, has become more popular at the expense of beach nourishment (Hamm et al., 2002; Hanson et al., 2002). Nevertheless, it is not immediately clear that the added sediment will actually be redistributed as desired. Shoreface nourishments are usually placed in depths of 4–8 m and have volumes of ~ 1 to 2×10^6 m^3 (Johnson et al., 2001; Grunnet et al., 2004; van Duin et al., 2004). The alongshore length scale is often of the order of several kilometres. Lee and feeder effects have both been observed in the field. The lee effect refers to the increased wave dissipation over the nourishment, which leads to a decrease in wave action in the lee of the nourishment and thus to a reduced longshore transport of sediment. Thus, for oblique wave incidence the longshore transport is reduced in this region, causing sediment convergence at the upstream nourishment end and divergence at the downstream end. For pure normal incidence there is a possibility of the generation of set-up currents and subsequent erosion in lee of the nourishment if there is substantial breaking on the nourishment. The feeder effect refers to cross-shore (onshore) supply of sediment from the nourishment to the shore

* Corresponding author. Tel.: +44 115 951 4164; fax: +44 115 951 3898.
E-mail address: Nick.Dodd@Nottingham.ac.uk (N. Dodd).
[1] Now at Cefas, Pakefield Road, Lowestoft, NR33 0HT, UK.

0378-3839/$ - see front matter © 2006 Elsevier B.V. All rights reserved.
doi:10.1016/j.coastaleng.2006.11.006

(Grunnet et al., 2004). This feeder effect is generally (but not always) the objective of the nourishment, but field studies show various behaviours. Shoreface nourishments on a barred beach generally become part of the dynamic bar system (van Duin et al., 2004; Grunnet and Ruessink, 2005), leading to complex morphological evolution in time.

Morphological evolution of a nourishment is essentially driven by two effects: i) the transport due to wave skewness and undertow and ii) transport due to the longshore current and the horizontal circulation (rip cells). Here we focus on the second mechanism and, in particular, on the horizontal circulations, as we assume waves approach perpendicular to the coast. Thus we assume that in the absence of alongshore gradients there would be no net transport. In other words, gradients in wave energy and wave set-up, due only to alongshore gradients caused by the nourishment, drive a horizontal circulation with onshore flow over the shoals and offshore flow over the channels in between. This is the only source of sediment transport in our study.

Recently it has been suggested (see Roelvink et al., 2005) that short scale nourishments might be more effective. Observations indicate that a large nourishment amplitude and short alongshore length scale enhance diffusion (Hamm et al., 2002), and that shoreward sediment transport is strongest at the alongshore edges of a nourishment (see for instance Johnson et al., 2001). Short scale nourishments could therefore optimise this effect and enhance onshore movement of sediment. On the other hand, they may also lead to the generation of strong rip currents, which can reverse that onshore movement by bringing a large amount of sediment seaward.

This suggestion was examined by Koster (2006), who found, using a numerical model study, that a nourishment of alongshore length 200 m and with spacing of 500 m between each nourishment had the most apparent beneficial effect: an increase of 175–300% in effectiveness over a traditional nourishment.

It is in this kind of situation, where rip currents and their onshore return flow may be crucial, that our study, which neglects undertow and wave skewness, may be particularly relevant for real shoreface nourishments. Furthermore, in addition to their morphological effect on the nourishments, rip currents also endanger swimmer safety.

A lot of questions remain about the effectiveness of shoreface nourishments due to their recent application history. Common questions include where to place the nourishment in the cross-shore direction, what length scale and nourishment height should be used (see Klein, 2005), the effect of nourishments with a different grain size from that of the coastal system in which they are placed, and the long-term evolution of nourishments (see Grunnet et al., 2004; Grunnet and Ruessink, 2005, for state of the art studies).

More fundamentally, it is not obvious what the effect of a nourishment will be on the overall beach stability, or how the hydro-morphodynamic system will respond to such a perturbation. Most numerical studies have used comprehensive numerical models to examine the fate of a nourishment over weeks or months (see Grunnet et al., 2004; Grunnet and Ruessink, 2005), in which cross- and alongshore processes are represented. Such an approach is highly desirable for practical purposes, and has shown much promise. However, the comprehensive nature of these kinds of model studies can also obscure more fundamental processes that are taking place. This is so partly because it is not always clear what physical processes are prevailing, cross-shore or alongshore for instance, or perhaps a few terms in the governing equations. These questions can be answered to some degree by switching off various terms and therefore isolating others in the modelling study. Pure numerical effects (e.g. numerical diffusion or dispersion, see Hudson et al., 2005) are more difficult to isolate, however. It is also much more difficult in such modelling studies to identify what are free and forced motions (see Dodd et al., 2003), i.e. what is the 'free' behaviour of the natural system, and what is due, for instance, to an engineering intervention.

In this paper we investigate the linear evolution of a series of shoreface nourishments along a straight coastline bordering a plane beach. To do this we first isolate the fundamental morphodynamical modes by means of a linear stability analysis of the beach to look at the types of likely behaviour. A morphodynamical mode is defined here as a spatial bed pattern (and accompanying flow pattern) with an associated growth rate. The physical system allows for growth of certain patterns (positive growth rate) and decay of other patterns (negative growth rate). Usually the former is of interest, because they may indicate a likely state to which the equilibrium will evolve. Here we consider all modes. We then express the nourishments as perturbations of the hydro-morphodynamic system using these modes and calculate the linear evolution of them. The purpose is to examine the subsequent evolution of the nourishments in terms of their constituent modes and their implications for nourishments and for nourishment dimensions. This projection method has been applied by De Swart and Calvete (2003) to study the nonlinear evolution of human interventions on shoreface-connected sand ridges (see also Calvete and De Swart, 2003). Linear evolution of morphological features using linear modes has also been studied by Roos et al. (2005). This approach has not been used before to study shoreface nourishments and nourishment evolution, and offers the possibility of a better understanding of the dynamical evolution of shoreface nourishments. Our study therefore has particular relevance in light of the work of Koster (2006), and also of Klein (2005), who also performed an idealised study of the effect of the length scale of nourishments on subsequent nearshore morphological change. We limit ourselves here to normal (random) wave incidence in order to develop and illustrate the method, but the approach is applicable to oblique incidence too.

In the next section we give the theoretical framework. This is followed by the examination of the morphodynamical modes, a detailed example of the procedure and then the analysis of the temporal behaviour of nourishments of different length scales. Finally, a discussion and some conclusions are presented.

2. Model description

The model is based on the wave- and depth-averaged shallow water equations, complemented by wave energy and phase equations and a bed evolution equation. The model geometry is

indicated in Fig. 1. Quasi-steady flow conditions are assumed and the spatial coordinates are (x, y), representing the cross- and alongshore directions, respectively, and t is the morphodynamical time coordinate. Standard expressions are adopted for the wave radiation stress, turbulent Reynolds stress, phase speed, group velocity, intrinsic and absolute frequency and the wave orbital velocity (see Mei, 1989). Wave dissipation follows the description of Thornton and Guza (1983) for random wave dissipation. Sediment transport follows the formulation of Soulsby–Van Rijn (see Soulsby, 1997), which is a total load formula for combined transport by waves and currents. The current in our formulation is depth-averaged. Furthermore, the effect of the waves in the Soulsby–Van Rijn formulation is just to stir the sediment but not to cause a net transport in the absence of currents. Thus, our sediment transport description is suitable for rip current circulation but does not include undertow and wave skewness effects. This type of formulation has commonly been adopted to study morphodynamic evolution when alongshore gradients exist (see, for instance, Deigaard et al., 1999). Please see Calvete et al. (2005) for model details.

2.1. Linear stability analysis

Following the standard procedure for linear stability analysis the variables are split into an equilibrium part plus a perturbation. The steady state dynamic equilibrium (i.e. the so-called basic state) is characterised by alongshore uniformity and spatially constant flow conditions, resulting in a zero sediment flux. Effects of bed slope are neglected in the equilibrium state since, consistent with our sediment transport formulation, it is assumed that the offshore transport due to slope effects and undertow is compensated by onshore transport due to wave asymmetry. Thus, the equilibrium bed is imposed as a plane, alongshore uniform beach (1:50 slope). The accompanying cross-shore free surface, velocity, wave energy and wave phase profiles are calculated from the equations. Constant offshore wave conditions are assumed. Here we take $H_{\mathrm{rms},\infty}=3$ m and $T_{\mathrm{p},\infty}=10$ s (for normal incidence). Note that it is important to assess how long these constant driving conditions are likely to be present. We estimate that these conditions may pertain for approximately 2 days per year, based on wave data for the Dutch coast (see http://www.golfklimaat.nl).

Next, a small perturbation is introduced onto the equilibrium state and the model equations are linearised with respect to that perturbation. Since the coefficients of the linearised equations are independent of y and t any solution for the perturbation is an expansion in solutions which depend exponentially on such

$$h' = \mathrm{Re}\{h(x)e^{\sigma t+iky}\}, \tag{1}$$

where h' represents the bed perturbation and $h(x)$ is its cross-shore profile, σ its growth rate and k the alongshore wavenumber. The wavenumber can be freely chosen and, for each choice, solving the equations for the growth rate and cross-shore profiles of the perturbations (i.e. $h(x)$ and the equivalents for free surface, velocity, wave energy and wave phase) poses an eigenvalue problem. The cross-shore profiles are the eigenfunctions and the growth rate is the eigenvalue. Thus for each choice of $k=k_j$ a set of M_j solutions are found, with growth rates σ_{mj} and cross-shore patterns h_{mj} $(x)(m=1, 2,\ldots, M_j)$. Actually, the real part of σ_{mj} is the proper growth rate and its imaginary part is the alongshore migration rate. Note that the number of modes M_j is finite: increasing mode numbers correspond to patterns with increasing cross-shore zero-crossings, providing a limit when cross-shore length scales become of the same order as the grid spacing (i.e. physical modes and numerical modes can no longer be distinguished). The wavenumbers are assumed to be real so that the eigenmodes are rhythmic in the alongshore direction. The eigenmodes and associated eigenvalue are called the modes of the system. Thus, modes (patterns) are found which can grow (positive growth rate) or decay (negative growth rate). The linear stability model MORFO60 (Calvete et al., 2005) is used to determine these linear eigenmodes and their structure is discussed in Section 3.1. The pattern with the largest, positive growth rate of all applied wavelengths will dominate the temporal evolution and is therefore the pattern to be expected in nature. Stability analysis has been applied successfully in coastal morphological studies (see Dodd et al., 2003), and many coastal bathymetries are characterised by alongshore rhythmicity.

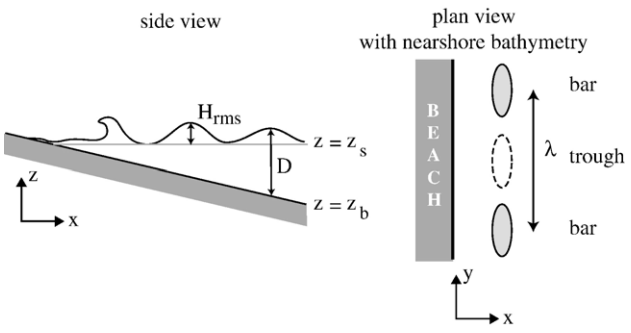

Fig. 1. Model geometry and variables.

2.2. Projection technique

We now consider a shoreface nourishment defined by $h=h_{\mathrm{nour}}(x, y)$ with the assumption that it is alongshore periodic with wavelength $\lambda_1=2\pi/k_1$. A numerical routine will be applied to complete the projection, therefore we will use $\mathbf{x}$, $\mathbf{y}$ instead of x, y from now on, where bold characters indicate vectors. The nourishment function $h_{\mathrm{nour}}(\mathbf{x}, \mathbf{y})$ is decomposed in the alongshore direction into Fourier components based on the initial wavenumber, k_1, ($\mathbf{k}=\{k_1, 2k_1, 3k_1,\ldots\}$). This is done for each cross-shore location point:

$$h_{\mathrm{nour}}(x_i,\ \mathbf{y}) \rightarrow \mathcal{F}(x_i,\ \mathbf{k}) \quad \text{for all } x_i \text{ in } \mathbf{x}. \tag{2}$$

Next, the cross-shore dependence of the Fourier amplitudes is projected onto the linear modes h_{mj} of the system:

$$\mathcal{F}(\mathbf{x},\ k_j) \simeq \widetilde{\mathcal{F}}(\mathbf{x},\ k_j) = \sum_{m=1}^{M_j} a_{mj} h_{mj}(\mathbf{x}) \quad \text{for all } k_j \text{ in } \mathbf{k}. \tag{3}$$

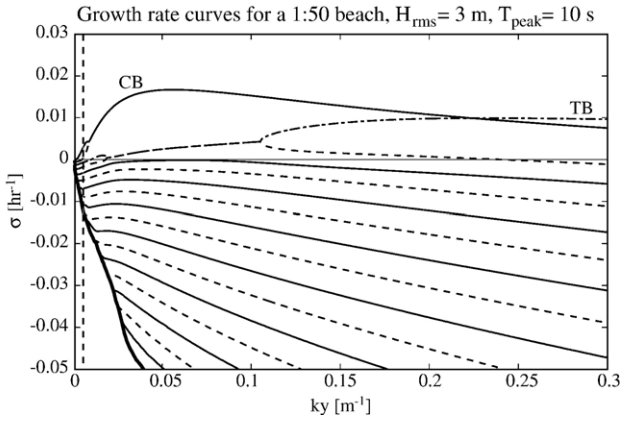

Fig. 2. Growth rates for a plane beach (default geometry, 1:50 beach) and normal wave incidence with $H_{\mathrm{rms},\infty}=3$ m, $T_{\mathrm{peak},\infty}=10$ s. The dashed vertical line indicates the wavenumber $k=0.004$ m^{-1}. Modes are plotted as solid and dashed lines alternatively, while the envelop mode is shown by the thick line.

The Fourier amplitudes a_{mj} are determined by a numerical programme using a Galerkin projection. The projections $\widetilde{\mathcal{F}}(x,k_{\mathrm{j}})$ then replace the original amplitudes and the inverse Fourier transform yields an approximation of the original nourishment function in terms of the modes of the system. We refer to this function as the projected nourishment. Thus the nourishment is reconstructed as $\tilde{h}$, with

$$\widetilde{h}_{\mathrm{nour}}(\mathbf{x},\ \mathbf{y}) = h_0(\mathbf{x}) + \sum_{j=1}^{N}\left(\sum_{m=1}^{M_{\mathrm{j}}} a_{\mathrm{mj}} h_{\mathrm{mj}}(\mathbf{x}) e^{ik_{\mathrm{j}}y}\right), \tag{4}$$

$$k_{\mathrm{j}} = jk_1$$

where the values of the amplitudes a_{mj} are the initial conditions and

$$h_0(\mathbf{x}) = \frac{1}{\lambda_1}\int_0^{\lambda_1} h_{\mathrm{nour}}(\mathbf{x},\mathbf{y})d\mathbf{y} \tag{5}$$

is the alongshore mean, corresponding to $k=0$. It follows from the linearised model equations that any alongshore uniform perturbation given to the equilibrium state remains constant in time. This is a consequence of our sediment transport formulation which disregards undertow and wave skewness effects, and the fact that nonlinear interaction has not been taken into account. Therefore, since the amplitudes of the modes evolve like $e^{\sigma mjt}$ the reconstructed nourishment will evolve as:

$$\widetilde{h}_{\mathrm{nour}}(\mathbf{x},\mathbf{y},t) = h_0(x) + \sum_{j=1}^{N}\left(\sum_{m=1}^{M_{\mathrm{j}}} a_{\mathrm{mj}} h_{\mathrm{mj}}(\mathbf{x}) e^{\sigma_{\mathrm{mj}}t+ikjy}\right). \tag{6}$$

Note that the Fourier amplitudes a_{mj} are the initial amplitudes ($t=0$) of the modes mj. Since the alongshore mean, $h_0(\mathbf{x})$, does not affect the time evolution (with the linearised

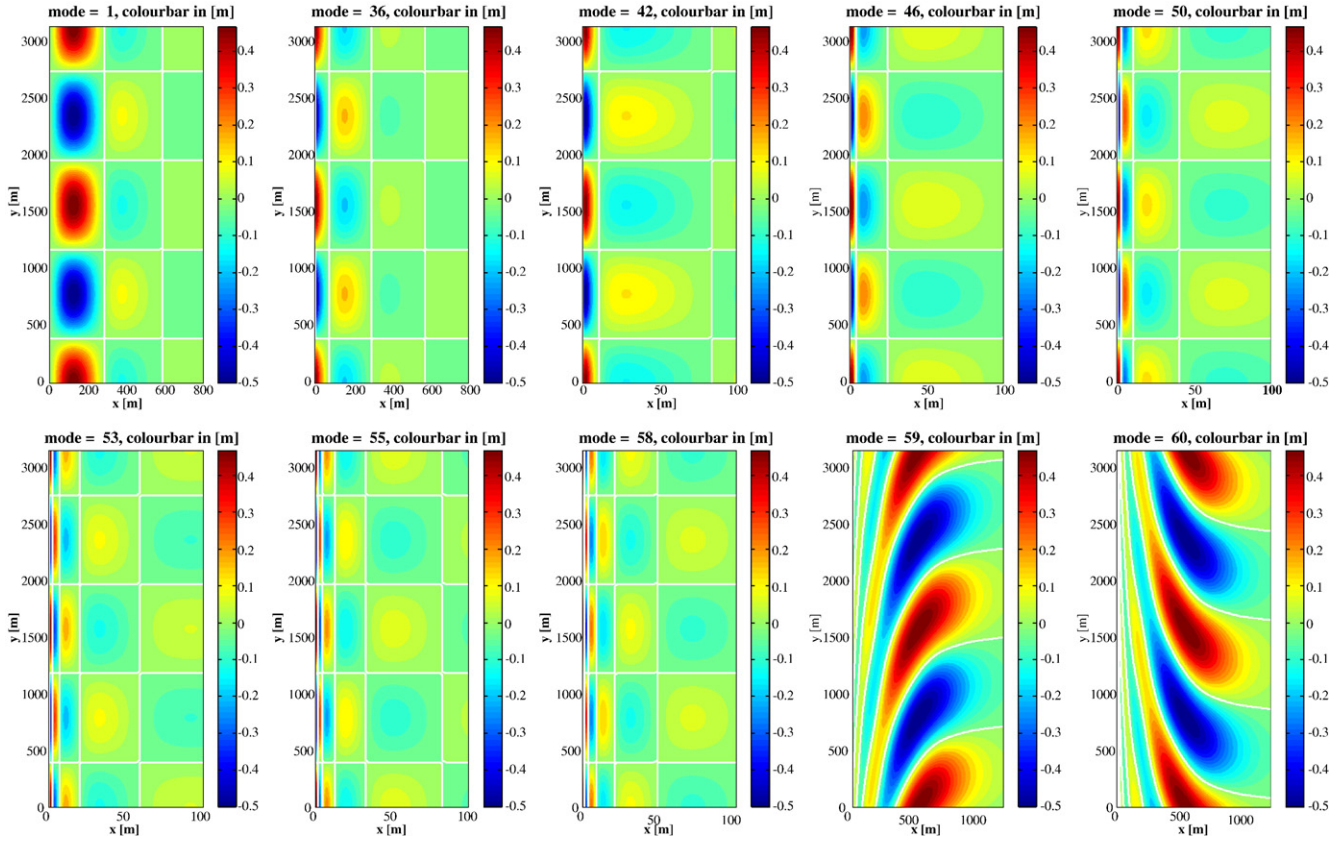

Fig. 3. Bed patterns found for $k_1=0.004$ m^{-1} (wavelength of 1571 m). Note the change in x-axis for the different plots. Plots are ordered (left to right, top to bottom) from largest positive to largest negative growth rates.

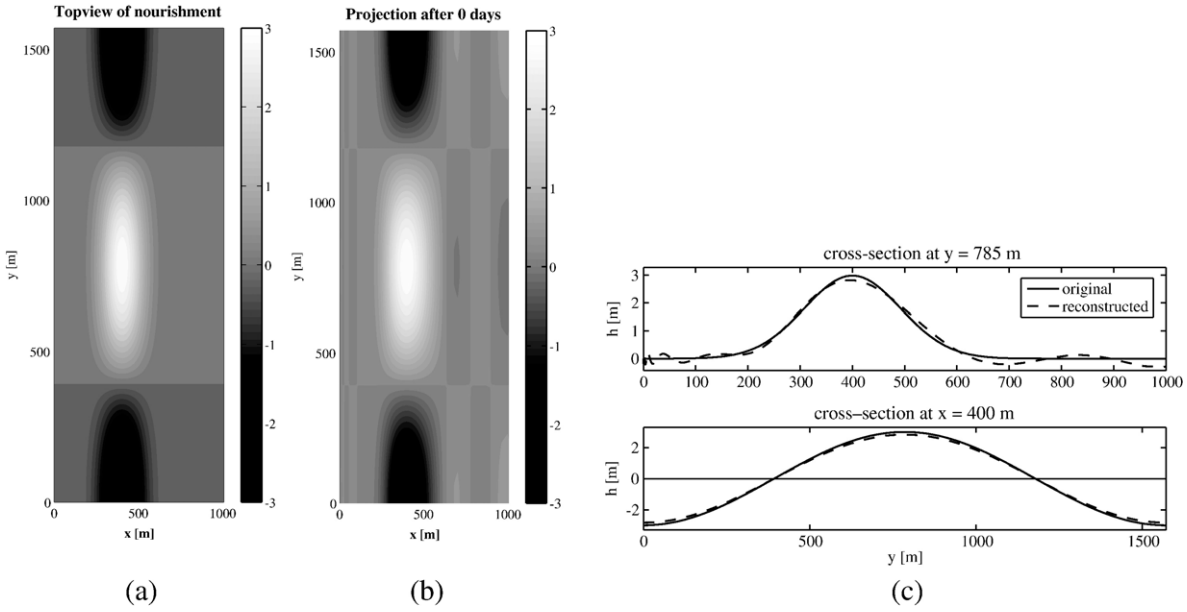

Fig. 4. Comparison for a long scale sinusoidal nourishment: (a) plan view of original nourishment, (b) plan view of projected nourishment, (c) cross-shore fit (top) and alongshore fit (bottom). $k_1=0.004$ m^{-1}; $y_0=785.4$ m; $x_0=400$ m; $A=3$ m; $w_x=130$ m.

equations), we will hereinafter pay attention only to the zero-mean component or, in other words, we will only consider nourishments with zero-mean.

3. Modal structure and detailed projection

Default parameters include a grain size of 250 μm, wave period $T_{peak,\infty}=10$ s, $H_{rms,\infty}=3$ m (to stir up sediments in depths up to 4–8 m where the nourishments are placed: see Section 2.1) and normal wave incidence ($\theta_\infty=0°$).

3.1. Modal structure

Here we present in detail the modal structure (type of bedforms that can grow or decay for a certain alongshore wavelength). This analysis is usually limited to examining growing bed patterns only (see Calvete et al., 2005; Van Leeuwen et al., 2006); in contrast we consider here the full modal structure, i.e. growing and decaying modes. Fig. 2 shows the modal structure of the basic geometry presented in Section 2, i.e. a plane beach with a 1:50 slope. Growing modes are evident, corresponding to crescentic patterns (CBs) and transverse bars (TBs) (see Van Leeuwen et al., 2006). Bifurcations are also observed, with two separate solutions that are complex conjugates for a range of alongshore wavenumbers. These complex conjugates modes represent the up- and downstream orientated patterns for oblique wave incidence. In the limit of normal incidence, considered here, they become spatially equal patterns with opposite migration rates. Why this only occurs for certain values of k is not clear. All growing modes (i.e. those that have a positive growth rate for some range of k) show this behaviour; decaying modes show no physical bifurcation behaviour.

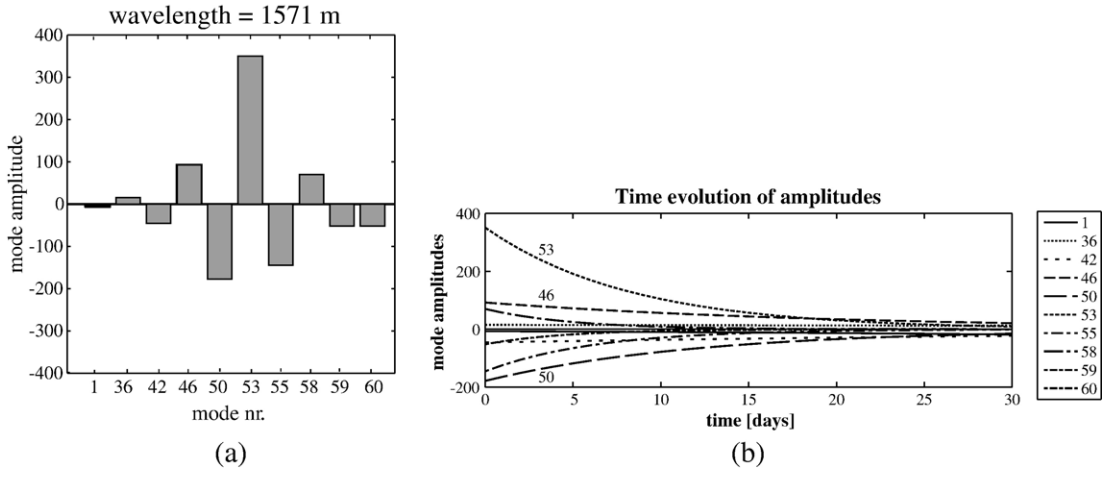

Fig. 5. (a) Projection amplitudes for $k=k_1=0.004$ m^{-1}. Black bars represent growing modes while gray bars indicate decaying modes. (b) Time evolution of projection amplitudes for $k=k_1=0.004$ m^{-1}.

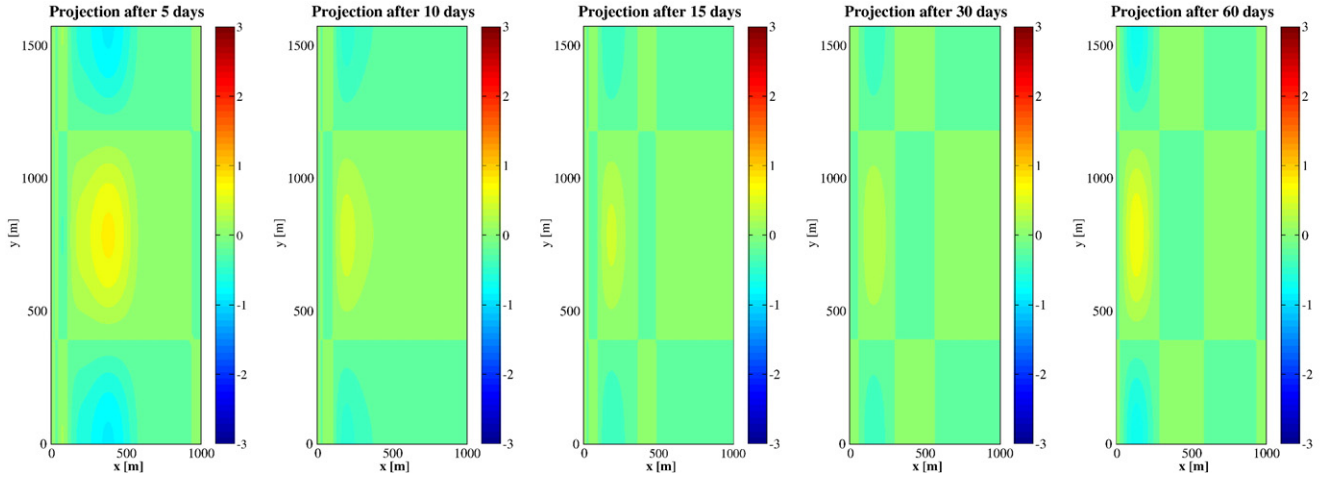

Fig. 6. Plan view of bed for a sinusoidal nourishment with $k_1=0.004$ m^{-1}: time evolution of projected nourishment (the time intervals change from left to right).

To study the patterns associated with these modes we show all patterns found for $k=0.004$ m^{-1} ($L_y=1571$ m). Nine modes are found for this wavelength, including a (decaying) complex conjugate mode. In Fig. 3 we show all eigenmodes (perturbation bed patterns) obtained for this wavelength down to the limit of model resolution from largest to smallest growth rate. Note that the plane sloping beach should be added to these profiles to obtain the total bed pattern. The steep downgoing curve of Fig. 2 (for small wavenumbers) is the decaying complex conjugate pair (Fig. 3, modes 59 and 60), which has a maximum at a substantial distance offshore. The other patterns (Fig. 3 modes 1 to 58) correspond to growing (mode 1) and decaying modes (36–58) with progressively increased numbers of zero-crossings and shoreline confinements (shoreward shifts). These decaying modes are the more horizontal lines in the lower part of Fig. 3. The modes are identified by their output number from the model (sorted on growth rate): the modes from output numbers not shown are artificial solutions due to the numerical scheme. The maximum bed perturbation is located in the surf zone or just outside of it (mirroring effect).

All patterns show a shoreward shift (of cross-shore maximum bed height) for increasing k.

Thus we hypothesise that each mode is characterised by a viability wavelength. Efficiency (i.e. geometry) dictates that along- and cross-shore length scales cannot be too dissimilar, as the patterns are driven by 2D circulation cells. The offshore extent of a mode is limited by the forcing conditions necessary to maintain its number of zero-crossings, so for each mode there is a maximum alongshore length scale above which the pattern can no longer exist. Thus patterns that cover a large cross-shore extent (note that this includes both mode 1 and the offshore mode, which effectively form an envelope of the others) can exist for larger wavelengths (smaller k). Patterns that are spatially restricted in the cross-shore direction therefore need smaller wavelengths (larger k) to be viable. Thus, more modes appear as the wavenumber becomes larger. The offshore mode is a large pattern, which has its maximum bed perturbation situated well outside the surf zone. For increasing k it does show a decrease in cross-shore extent and a shift of the maximum bed perturbation towards the shore, until it can no longer be distinguished from other modes. Increasing oscillations in the cross-shore direction eventually lead to increasing numerical errors in the stability analysis (physical resolution), such that modes can no longer be regarded as physical. Why the offshore mode appears as the envelope of the surf zone modes is not clear.

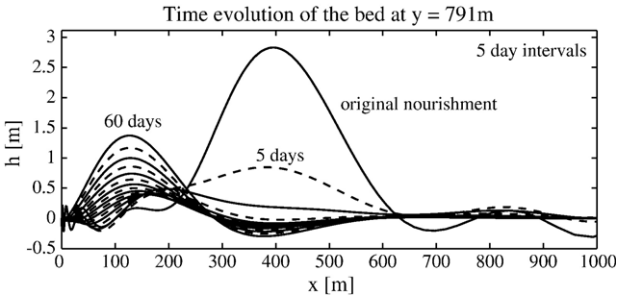

Fig. 7. Time evolution of the cross-section for the sinusoidal nourishment with $k_1=0.004$ m^{-1}. The top line indicates the original nourishment, with subsequent profiles in 5 day intervals. Profiles are shown as solid and dashed lines alternatively.

3.2. Projection of a nourishment

First, the nourishment itself needs to be defined. Two different shapes are used: a sinusoidal and an elongated Gaussian nourishment. The name refers to the shape in the alongshore direction, with a Gaussian curve prescribed in the cross-shore direction in both cases:

$$\text{SINUSOIDAL} \quad h_{\text{nour}} = -Ae^{-\left(\frac{x-x_0}{w_x}\right)^2}\cos\left(\frac{2\pi y}{L_y}\right), \tag{7}$$

$$\text{GAUSSIAN} \quad h_{\text{nour}} = Ae^{-\left(\frac{x-x_0}{w_x}\right)^2}e^{-\left(\frac{y-y_0}{w_y}\right)^2} \quad \text{for } 0\le y\le y_1 \text{ and } y_2\le y\le L_y \tag{8}$$

$$= Ae^{-\left(\frac{x-x_0}{w_x}\right)^2} \quad \text{for } y_1<y<y_2. \tag{9}$$

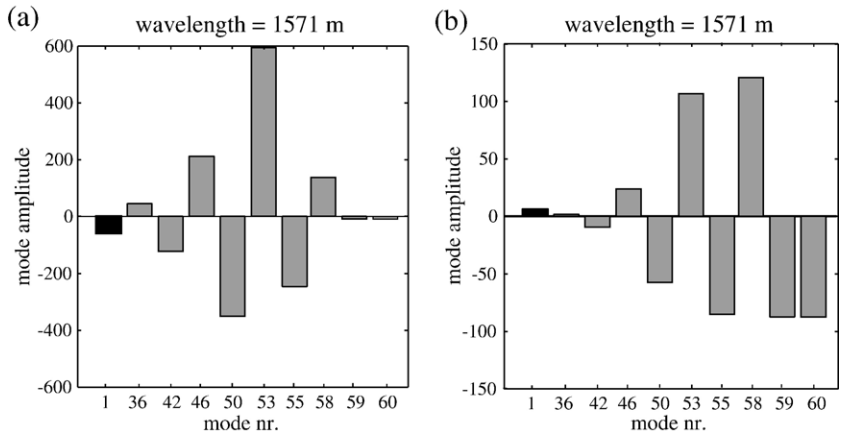

Fig. 8. Projection amplitudes for $k=k_1=0.004\ \mathrm{m}^{-1}$ for a nourishment 300 m offshore (left) and 500 m offshore (right). Black bars represent growing modes while gray bars indicate decaying modes.

Here A is the amplitude of the nourishment, $w_{x,y}$ is the width in the cross- and alongshore direction of the Gaussian component, x_0 is the cross-shore location of maximum amplitude and L_y the basic alongshore wavelength. This wavelength corresponds to the initial wavenumber $k_1=2\pi/L_y$ of the sinusoidal nourishment. The Gaussian nourishment (see above) is split in

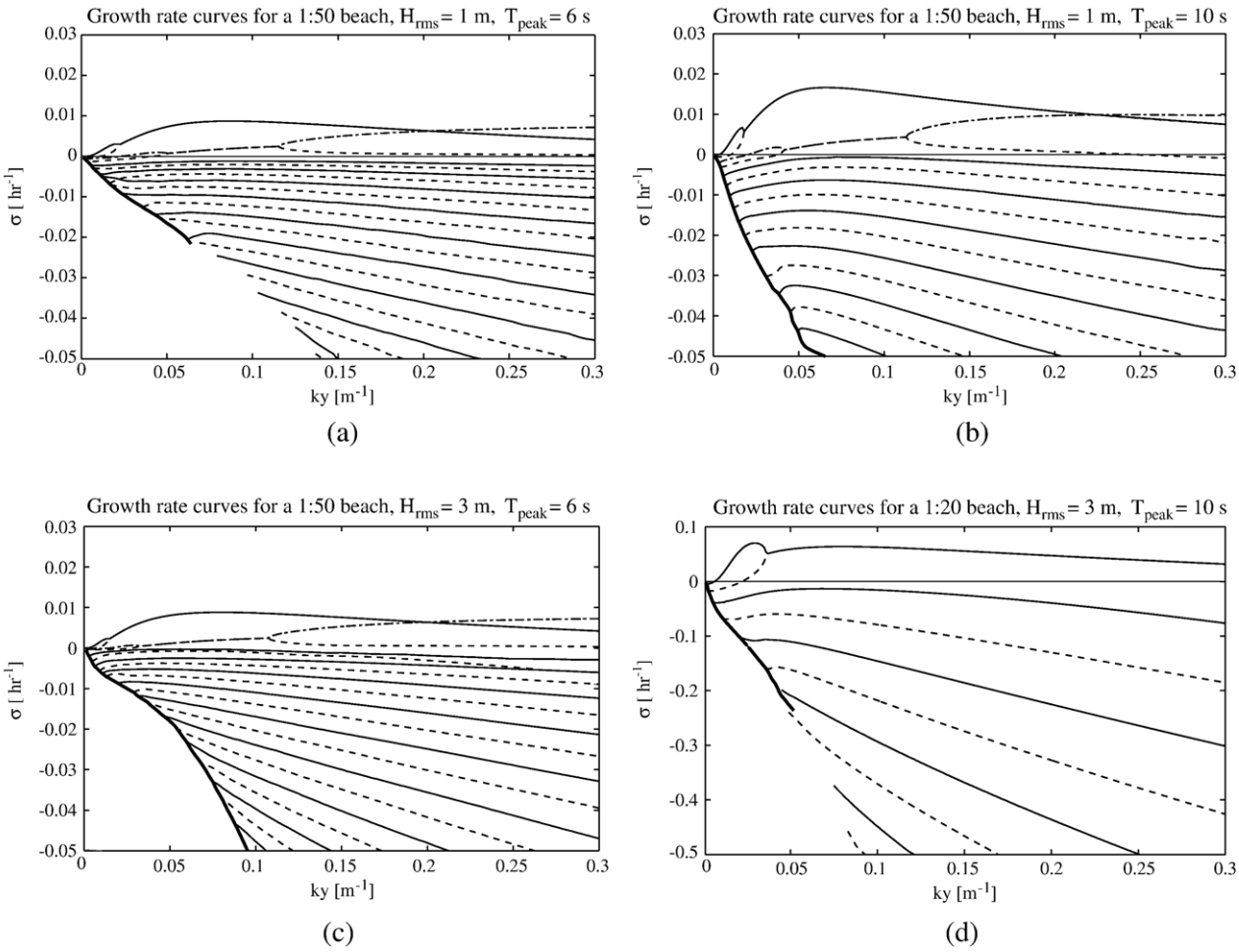

Fig. 9. Growth rates for a plane beach and normal wave incidence with (left to right, top to bottom) (a) default geometry and decreased wave height and peak wave period (1:50 slope, $H_{\mathrm{rms},\infty}=1$ m, $T_{\mathrm{peak},\infty}=6$ s), (b) default geometry and decreased wave height (1:50 slope, $H_{\mathrm{rms},\infty}=1$ m, $T_{\mathrm{peak},\infty}=10$ s), (c) default geometry and decreased wave period (1:50 slope $H_{\mathrm{rms},\infty}=3$ m, $T_{\mathrm{peak},\infty}=6$ s) and (d) default forcing and a steep beach (1:20 slope, $H_{\mathrm{rms},\infty}=3$ m, $T_{\mathrm{peak},\infty}=10$ s). The modes are alternatively drawn as solid and dashed lines. The thick line is the envelop mode.

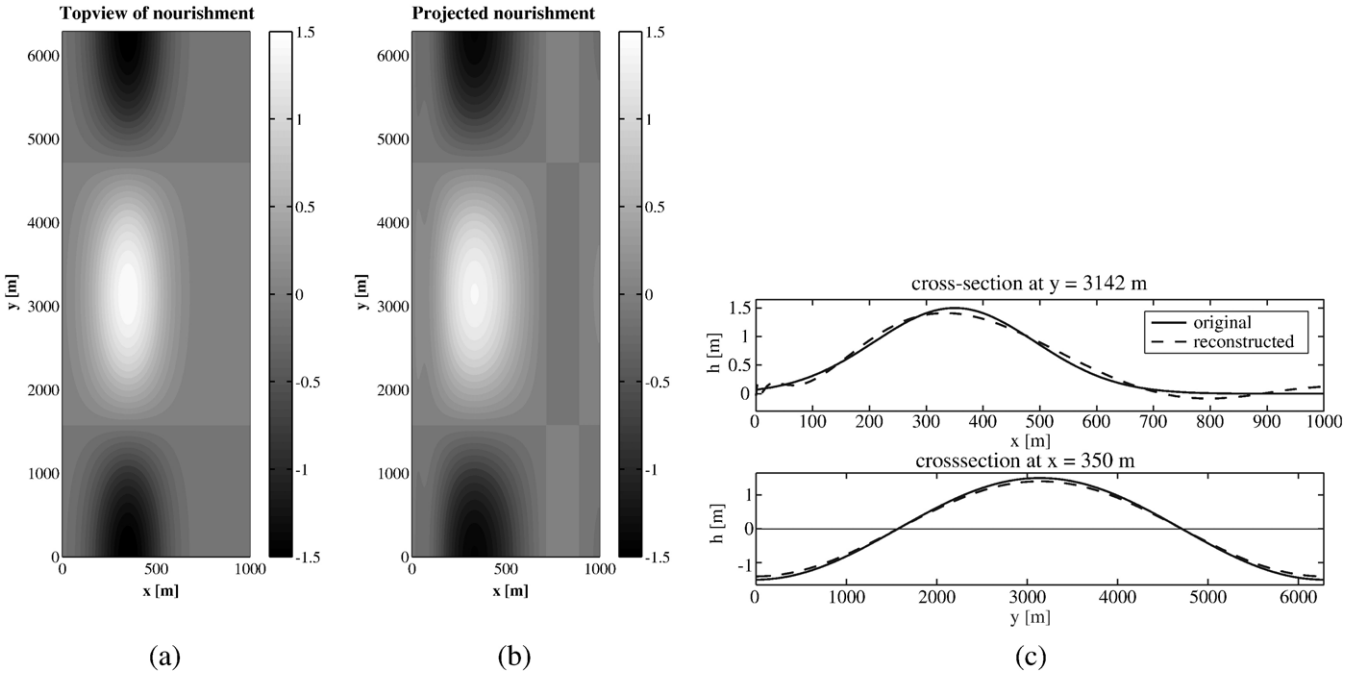

Fig. 10. Comparison for a large scale sinusoidal nourishment: (a) topview of original nourishment, (b) topview of projected nourishment, (c) cross-shore fit (top) and alongshore fit (bottom). Reconstruction with decaying modes only. x_0=300 m, w_x=200 m, A=1.5 m, k_1=0.001 m^{-1}.

the alongshore direction to allow for an elongated section that more realistically reproduces a shoreface nourishment. The sinusoidal nourishment already meets these requirements. The choice of y_1, y_2 thus allows us to produce isolated nourishments separated by a very shallow trough region in between ($y_2-y_1 \ll L_y$), or long, uniform nourishments separated by narrow, deep troughs ($y_2-y_1 \sim L_y$). y_0 is the centre of the nourishment in the alongshore direction for the fully Gaussian nourishment.

To illustrate the projection procedure we recreate a sinusoidal nourishment with an initial wavelength of 1571 m (k_1=0.004 m^{-1}; y_0=785.4 m). The Fourier decomposition includes patterns down to 20 m in the alongshore direction (k=0.3 m^{-1}), below which they are not included in the analysis. Here the projection uses only modes with wavenumber k_1, as the nourishment is sinusoidal. Fig. 4 shows the original sinusoidal nourishment, the projected nourishment and the fit in the cross-shore and alongshore directions. Note that x_0=400 m, and that the nourishment is therefore located in water originally of 8 m depth. With an amplitude of 3 m and a width of 130 m this leaves a depth over the bar of 5 m in this scenario. It is important to note, however, that the amplitude of the nourishment has no

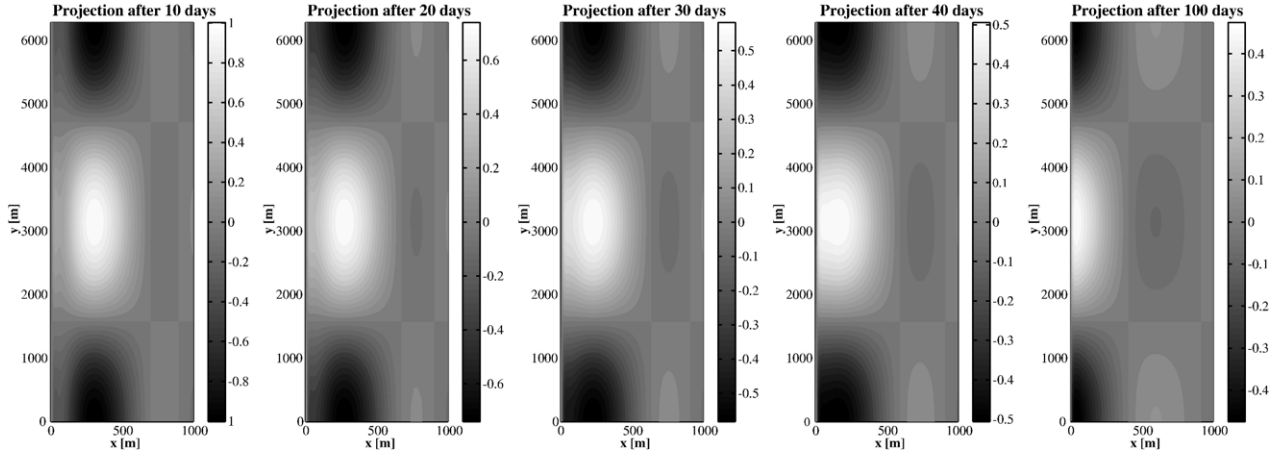

Fig. 11. Plan view of bed for a sinusoidal nourishment k_1=0.001 m^{-1}: time evolution of projected nourishment. Reconstruction with decaying modes only. Note the changing time step between adjacent figures and the change in bed height indicated by the colour bar.

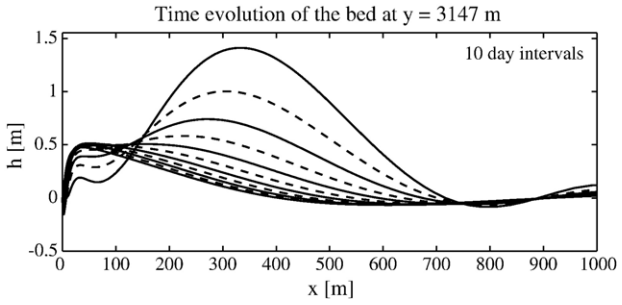

Fig. 12. Time evolution of the cross-section for the sinusoidal nourishment with $k_1=0.001$ m^{-1}. The top line indicates the original nourishment, with subsequent profiles in 10 day intervals, shown alternatively as solid and dashed lines.

impact on these decompositions and subsequent evolutions. The equilibrium bed is not included in the figures as this obscures the comparison. The original nourishment involves relocation of $\sim 0.35\times10^6$ m^3 of sand, consistent with actual nourishments considering its shorter alongshore length. It can be seen that the fit is generally good, with only small scale spatial oscillations near the shore indicating any significant deviation from the assumed form.

Fig. 5a shows the projection amplitudes, a_{m1} ($m=1,\ldots, M_j$), for this wavelength. As can be seen, the nourishment comprises mostly decaying modes of the initial wavelength (see Fig. 3 for these patterns). The offshore mode is no more strongly represented than the other modes due to its offshore location. Note, however, the equal amplitudes of this complex conjugate pair, due to their symmetry with respect to the nourishment. An implication of this is that if we can view a nourishment as an excitation of an alongshore periodic mode, it is likely to decay. The rate at which this will occur is dependent on the decay rates of the various modes of k_1 that comprise the projection, and thus on the length scale of the nourishment (see Fig. 2). Time evolution of the amplitudes $a_{m1}\, e^{\sigma m1 t}$ ($m=1,\ldots, M_j$) is shown in Fig. 5b, while the bed evolution is shown in Fig. 6 in topview. Note that only the evolution of the modes is shown, so that the equilibrium slope should be added for the total bed profile. The time evolution shows that, eventually, the growing mode (mode 1, see Fig. 3) becomes dominant. Fig. 7 shows the evolution of the cross-section at the location y_0 (middle of the y-axis). The exponential growth is clearly visible at $x\approx110$ m. This behaviour is inevitable given the existence of exponentially growing modes. However, the exponential growth is located shoreward of the nourishment and is the result of the unstable nature of the plane beach (basic state). As our interest lies in the diffusive behaviour of the nourishment, we will therefore eliminate growing modes henceforth from our projection technique.

Different cross-shore positions (x_0) of the nourishment lead to different projections in the cross-shore direction. Fig. 8 shows the amplitudes of the k_1 modes used in projections with $x_0=300$ m and 500 m. The same nourishment shape was used, so that depth over the bar varies with location. Note the increased use of the growing mode for the nourishment located 300 m offshore and the emphasis on the offshore mode for the nourishment at 500 m. The results illustrate the difference in mode wavenumbers that can be excited as a function of offshore location, leading to different temporal behaviour.

The modal structure of the beach will change for different wave conditions or a different slope. Fig. 9 shows the modal structure for a beach with decreased wave height and peak wave period (9(a)), decreased wave height forcing (9(b)), decreased peak wave period (9(c)), and for default forcing with a steeper beach profile (1:20) (9(d)). It can be seen that the offshore mode always forms an envelope of the other decaying modes, but also always eventually disappears as $k\rightarrow\infty$. Growth rates saturate for increasing wave height: here, saturation seems to have been reached for $T_{peak,\infty}=6$ s (a very small increase is observed) but not yet for $T_{peak,\infty}=10$ s (see Van Leeuwen et al., 2006, for a more thorough look at this). The decay rates, however, show variability even when the growing modes exhibit saturation. For

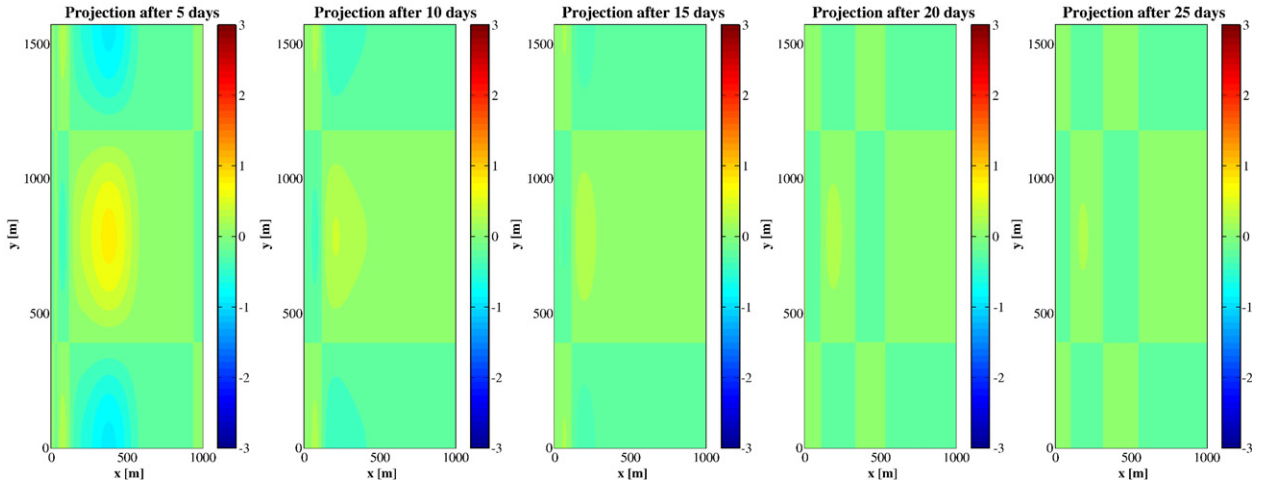

Fig. 13. Plan view of bed for a sinusoidal nourishment with $k_1=0.004$ m^{-1}: time evolution of projected nourishment.

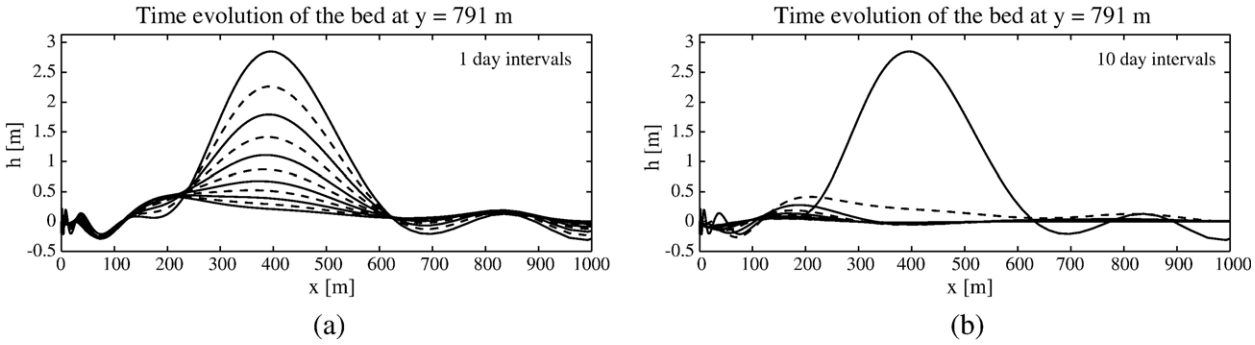

Fig. 14. Time evolution of the cross-section for the sinusoidal nourishment with $k_1=0.004$ m^{-1}. The top line indicates the original nourishment: (a) cross-profiles at 1 day intervals and (b) at 10 day intervals. Profiles are alternatively shown as solid and dashed lines.

increasing periods both growth and decay rates increase (cf. Fig. 2). Note, however, that for a fixed k the total number of modes for a particular bathymetry is about the same regardless of forcing. For example, for $k=0.05$ m^{-1} we have about 13 modes, excluding the offshore mode (Fig. 9(a)–(c)). For Fig. 2 this has increased to at least 15. In contrast, for a steeper beach (default conditions) growth and decay rates increase markedly and modes become more sparse (Fig. 9(d)).

4. Long scale nourishments

First, nourishments of alongshore scale $\mathcal{O}$(km) are considered. Studies of nourishments of this length scale can be found in Johnson et al. (2001), van Duin et al. (2004), Grunnet et al. (2004). Projection of a nourishment ($x_0=300$ m, $w_x=200$ m, $A=1.5$ m) with an initial wavelength of 6283 m ($k_1=0.001$ m^{-1}) shows a less good fit than that for the smaller scale nourishment of the previous section. This is due to the smaller number of modes found for this wavelength (see Fig. 2). Only decaying modes are found for $k=0.001$ m^{-1}. Fig. 10 shows the original sinusoidal nourishment and the projected nourishment. Here, $\sim 1.1\times10^6$ m^3 of sand was shifted in order to create the original nourishment. With an alongshore length scale of $\sim$2.5 km this nourishment is consistent with those applied in the field (van Duin et al., 2004; Grunnet and Ruessink, 2005). The fit between the original and projected nourishment is considered acceptable. The small number of modes found for this wavelength prohibits a further offshore placement of the nourishment. Fig. 11 shows the time evolution of the projected nourishment.

The time evolution shows decay accompanied by an onshore movement. Temporal evolution of the bed (without the

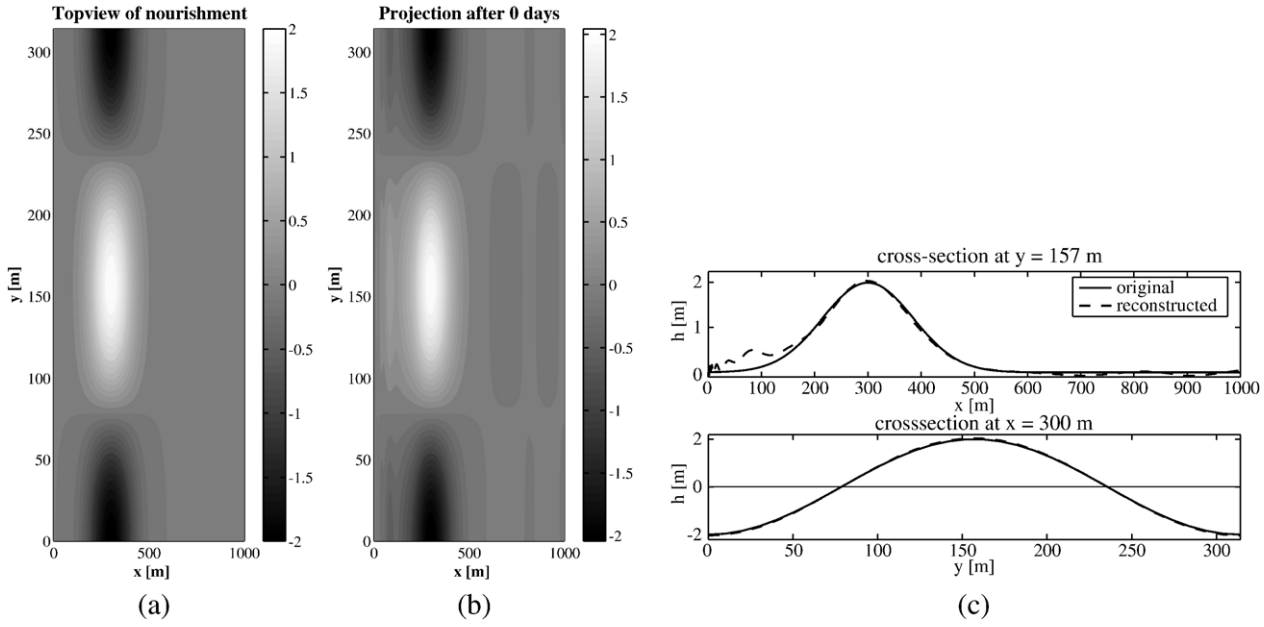

Fig. 15. Comparison for a small scale sinusoidal nourishment: (a) plan view of original nourishment, (b) plan view of projected nourishment, (c) cross-shore fit (top) and alongshore fit (bottom). $x_0=300$ m, $w_x=120$ m, $A=2.0$ m, $k_1=0.02$ m^{-1}.

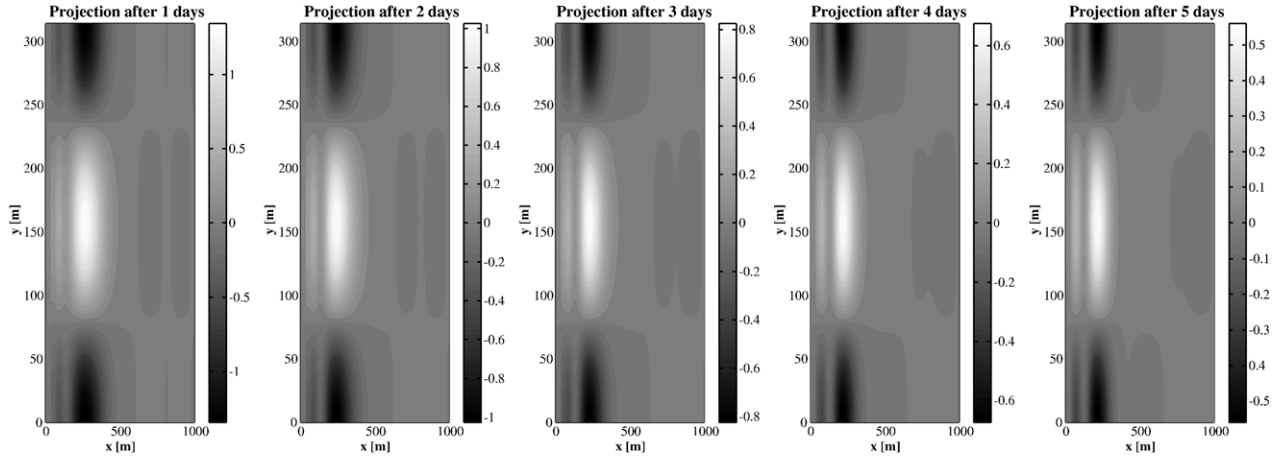

Fig. 16. Plan view of bed: time evolution of projected small scale sinusoidal nourishment. Note the decay as indicated by the decrease in maximum height of the colour bar.

equilibrium slope) is presented in Fig. 12 for cross-sections at different times. The slow decay of the nourishment is clearly visible. The nourishment moves slowly in the shoreward direction; this is due to the projection onto modes with different decay rates. Thus, as the nourishment decays in time in its original position other modes seem to grow as they are no longer balanced in the projection by the faster decaying modes. The apparent onshore migration of the nourishment is, it would seem, a desirable feature. The nourishment still possesses a substantial amplitude after 100 computational days (about one third of the original). However, this amplitude is already reached after 50 days, followed by very slow decay afterwards. Once again, we can relate our default forcing conditions to those on the Dutch coast, where they pertained for about two days per year. Therefore we may relate our 50 computational days to about 25 years of real time.

Fig. 13 shows the temporal behaviour of the nourishment of initial wavelength 1571 m (see the previous section), now using only decaying modes. Again, the equilibrium slope should be added for the full bed profile. Shoreward movement is once more apparent. After 5 days the original height of 3.0 m (above the equilibrium bed) has been reduced to ~0.8 m. It diminishes rapidly over only 20 days to a small fraction of its original size. Time evolution of the individual mode amplitudes is presented in Fig. 5. The nourishment decays over a period of 10 days to about a sixth of its original height. This is further shown in Fig. 14, which shows the cross-sectional evolution. We estimated previously that the energetic wave conditions pertain for only 2 days per year. This leads to an equivalent of 5 years evolution for the nourishment to reach a sixth of its original height if we neglect response in less energetic conditions. Again a shoreward movement of the nourishment is observed, although it is limited here to approximately 180 m offshore.

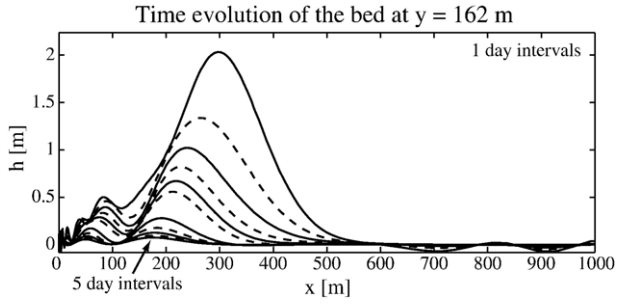

Fig. 17. Time evolution of the cross-section for the sinusoidal nourishment with $k_1 = 0.02\ \mathrm{m}^{-1}$. The top line indicates the original nourishment: cross-profiles at 1 day intervals. Profiles are shown as solid and dashed lines alternatively.

5. Short scale nourishments

Next we consider smaller scale nourishments, on the scale of $\mathcal{O}(100\ \mathrm{m})$. Roelvink et al. (2005) suggest that many small nourishments may be more effective than a large one. They envisioned a longshore row of small nourishments with large spaces in between, to reduce possible rip current effects and to discourage offshore transport of sediment. First, we consider a small sinusoidal nourishment. Fig. 15 shows the original and projected nourishment with an initial wavelength of $L_y = 314$ m or $k_1 = 0.02\ \mathrm{m}^{-1}$. The volume of the original nourishment is $\sim 0.043 \times 10^6\ \mathrm{m}^3$.

The temporal behaviour of the projected nourishment is shown in Figs. 16 and 17. The time evolution for this small scale nourishment shows a small shoreward movement. The rapid decay of this nourishment is typical of shorter scale nourishments (see Fig. 2).

A more realistic looking nourishment can be obtained by placing an isolated, small scale nourishment in a larger domain. These nourishments (as the system is alongshore periodic) would be close to those suggested by Roelvink et al. (2005). Thus we consider a nourishment of $\mathcal{O}(100\ \mathrm{m})$ in a region several kilometres long. This nourishment is defined as a Gaussian bump in both directions, with a constant extension in the alongshore direction of 100 m. Fig. 18 shows the original and projected nourishments for this case. Here $0.036 \times 10^6\ \mathrm{m}^3$ of sand was replaced to create the shoreface nourishment. The large alongshore length scale of the domain and relatively short length of the nourishment result in a more realistic nourishment,

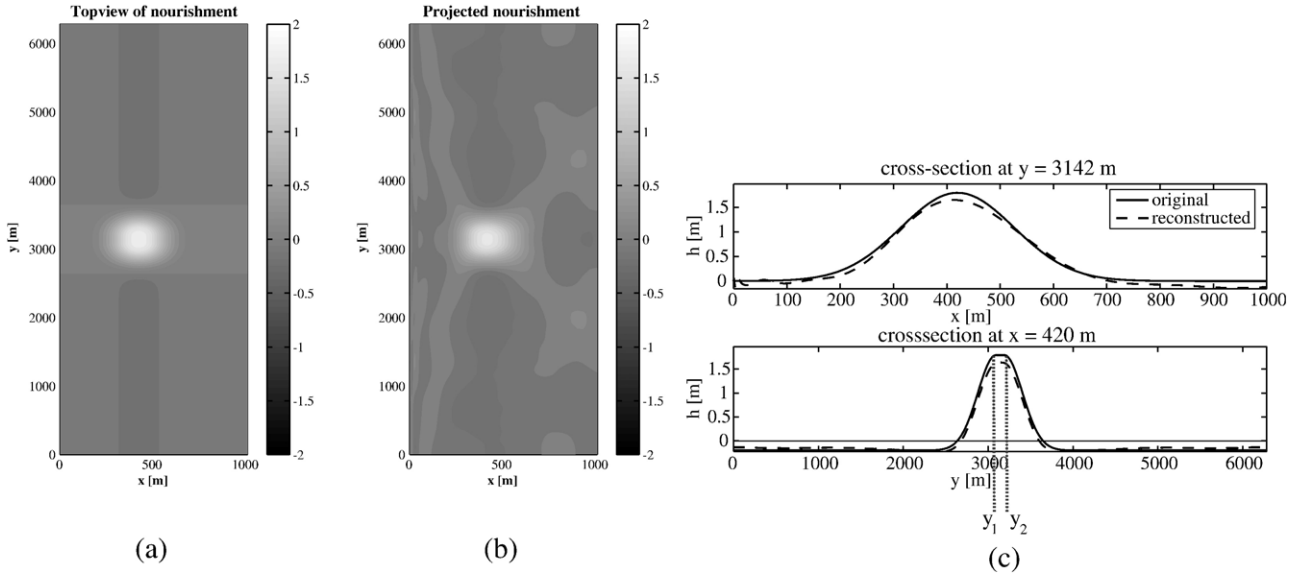

Fig. 18. Comparison for a small scale Gaussian nourishment: (a) topview of original nourishment, (b) topview of projected nourishment, (c) cross-shore fit (top) and alongshore fit (bottom). x_0=420 m, w_x=150 m, A=2.0 m, w_y=300 m.

although no sand is added to the system as a whole. Here, eight different wavenumbers are used for the projection. Fig. 19 shows the time evolution of the Gaussian shaped nourishment. This nourishment comprises several alongshore wavenumbers, leading to features of different length scales emerging. For this reason we show the time evolution only in topview. Here we observe a spreading of the nourishment, mainly in the alongshore direction, accompanied by a small inshore movement. The timescales show decay over 15 computational days to a bed height (of the perturbation) of 0.24 m. In real time this would indicate decay over 7.5 years to a sixth of the original height.

6. Discussion

The modal structure for a plane beach (see Figs. 2 and 9) indicates that longer (alongshore) scale nourishments will decay more slowly than their shorter scale counterparts. This slow decay is a robust feature of our long scale nourishments. It occurs because, for a long enough length scale, the decay rate of the decaying modes becomes very small. The nourishments also migrate shoreward as they decay. This occurs because the modes that initially comprise most of the nourishment decay at different rates. Careful inspection of Fig. 3, and Figs. 5 and 8 shows that nourishments sometimes contain a substantial contribution from the so-called offshore mode, but that they are more usually primarily composed of sums of higher order modes each with maxima in the surf zone, whose resultant surf zone-associated behaviour mostly cancels out. The shoreface nourishment thus comprises primarily, perhaps surprisingly, offshore portions of surf zone-associated modes. Significantly, shoreface nourishments, other than perhaps very short scale ones, are not composed of growing (unstable) modes. This is because these modes, which are comparatively few, have fewest

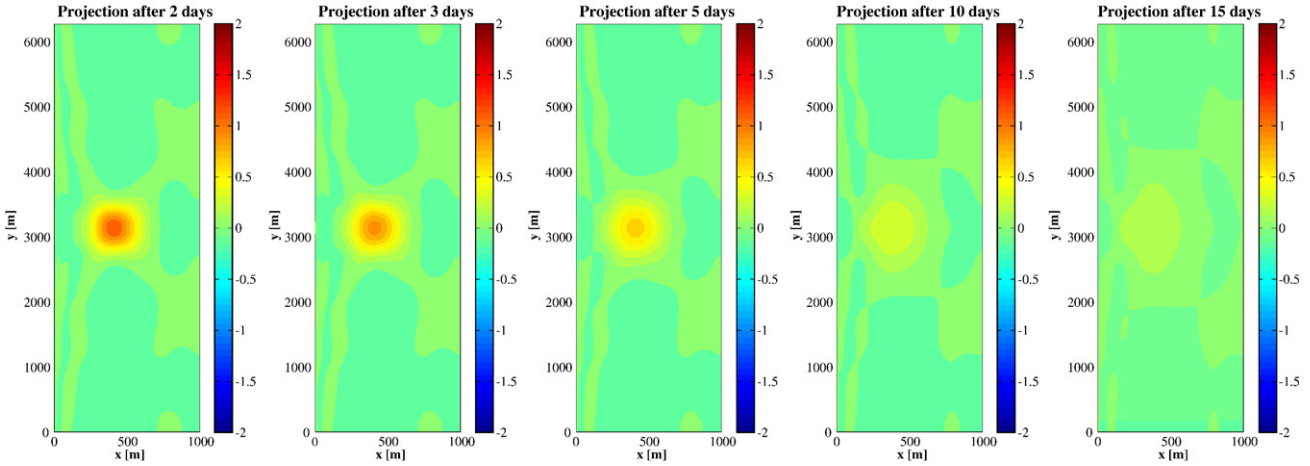

Fig. 19. Topview of bed: time evolution of projected nourishment for the small scale Gaussian nourishment case. Note that the time step between plots is not constant.

zero-crossings and are therefore strictly limited to the surf zone. The disturbing of this initial balance in the modes as they subsequently decay at differing rates leads to the onshore migration seen in the evolutions. Again, it is important to appreciate that, in long enough nourishments, all modes decay, but because of the different rates, the bed can rise locally. This migration can be deemed beneficial for a shoreface nourishment, because it corresponds to the deposition of sediment nearer the shore. This migration is also commonly observed in 'feeder berms' (see van Duin et al., 2004), which are shoreface nourishments, although it must be remembered that our study is limited to pure normal incidence so the classical lee effect due to local interruption of longshore sediment transport is not included here. The use of a zero-mean nourishment and the exclusion of growing modes will eventually lead to a return to the original state (without nourishment), but again, this would occur over a longer time scale.

So, decaying modes comprise the overwhelming majority of modes (see Figs. 2 and 9), and make up the nourishments themselves. All this means that shoreface nourishments are essentially decaying (diffusive) features, at least insofar as depth-integrated hydrodynamics are concerned. Ultimately, growing modes will come to dominate the evolution of the surf zone region as a result of the inherent instability of the basic state and, in a nonlinear model, of the nonlinear interaction between the evolution of the nourishment and the growing modes.

The decay rate (e-folding time) of the nourishments depends on the linear decay rates. But locally (see Figs. 12 and 14) this rate can vary substantially. A slow decay (long scale nourishments) is also likely to be beneficial for a nourishment, because it implies that 2DH morphohydrodynamics will not quickly rearrange the sediment, which will therefore primarily be moved by effects not considered here, i.e. the feeder effect. Thus, a shoreface nourishment located where cross-shore sediment transport is thought to be onshore may reasonably be expected to result in onshore sediment movement. Moreover, a nourishment that remains intact for some time will benefit from the lee effect.

It should be remembered, however, that at longer length scales the modal structure of the beach becomes more sparse. In our projections the implication of this is that we can only represent a limited range of offshore locations of a shoreface nourishment. A nourishment that is no longer expressible in terms of constituent modes of the 2DH morphodynamical system is an indication that the set of normal modes is not a complete set. In such cases, the time evolution of the nourishment could not be discerned from the constituent modes and would need a numerical integration of the (linearised) initial value problem. It is not surprising that the normal mode approach loses validity for very long nourishments since there will be little that distinguishes it from a new, alongshore uniform beach profile.

A nourishment that is not expressible in terms of constituent 2DH modes may also be inactive. As shown in Fig. 9 the beach modal structure, in particular that of the decaying modes, varies depending on wave forcing. Thus, a nourishment that decays in our default scenario (Fig. 2), could decay even more slowly under lower energy conditions, or, as mentioned above, no longer be expressible as such a perturbation, which under low enough energy conditions will mean inactivity of the nourishment. This interpretation prompted the estimate of a 'real' decay time based on how long our quite energetic forcing conditions are likely to pertain. The estimate here (2 days per year) probably leads to an overestimate of the decay times, but this kind of interpretation is likely to be necessary to give more realistic estimates of diffusion rates. For a steeper beach decay rates are substantially larger and modes more sparse, so that a more comprehensive physical description is more likely to be required. Note also that the richer modal structure at shorter length scales means that shorter scale nourishments are particularly likely to be expressible in our expansions. Our results here—that they will decay much more rapidly—seem robust therefore.

These results seem opposite to those of Koster (2006), who concluded that short scale, regularly spaced nourishments were beneficial compared to longer scale isolated ones. However, further research by Koster et al. (personal communications) has shown that multiple short scale nourishments suffer a decrease in their sediment trapping capability (due to decreased wave blocking) compared to longer scale nourishments. Their new study indicates that the most effective length scale of a shoreface nourishment is highly dependent upon local conditions. We note that the approach presented in this paper has more limitations than the traditional modelling approach of Koster (2006). First, the method is linear. The inherent limit of predictability this implies does not limit us, however, because we only seek the evolution, but our nourishments are of finite amplitude and therefore may not behave according to linear dynamics. Field results can show considerable nonlinear behaviour (van Enckevort et al., 2004). Therefore, our linear analysis must be viewed with some circumspection. Nevertheless, it is well known that linear theory does predict the (nonlinear) kinematics of natural morphodynamical pattern formation remarkably successfully, to the extent that finite amplitude patterns with linear characteristics can frequently be observed (see e.g. Damgaard et al., 2002; Reniers et al., 2004). Nevertheless, our analysis does assume that the nourishments must be small in some sense. It is difficult to know how restrictive this assumption is. A 3 m high nourishment in 8 m depth would seem substantial; a 1 m high nourishment perhaps could be termed small. Given that shoreface nourishment takes place offshore of the surf zone (i.e. in the deeper water of what is usually the shoaling zone) this assumption, while questionable, does appear to have relevance. Interaction between the nourishment and existing alongshore patterns (bars) is also not captured by the model as the basic state defines the modal structure on which the projection is based, thereby excluding alteration of the basic state due to the projection.

Interestingly, the study of Klein (2005) does appear to show some parallels with ours. Most of that study is of finite amplitude evolution of a short and long length scale nourishment about 400 m offshore and just seaward of an alongshore bar. After just 5 h (well within our linear evolution phase) both nourishments clearly begin to migrate onshore and exhibit some diffusion. This, it appears, is due to enhanced

breaking because modelling is 2DH; the result is bed level growth on the bar (onshore of the nourishment) and decay over the original nourishment. Laterally, however, there is diffusion, although indistinguishable between the two length scales. We further note that the short scale nourishment (800 m in Klein (2005)) is only eroded at its original location and "moved" onshore, along with some diffusion, but that the longer scale nourishment is affected this way at the ends only, due to the circulation cells that appear (Fig. 5.17 of Klein, 2005), and are then subsequently modified (Fig. 5.25 of Klein, 2005). In Klein's work the centre of the nourishment is actually depositional after 5 h, but less strongly than the edges are erosional, and for a longer nourishment it seems likely that the centre would be less active due to 2DH effects; thus the (3D) feeder effect alone modifies the nourishment. This finding–that longer nourishments therefore take longer to diffuse away–is consistent with our findings. We also note in Klein's experiments shorter length scale features growing at the shoreward bar after a short time (Fig. 5.25 of Klein, 2005), in effect being excited by the nourishment. These are equivalent to the growing modes (see Figs. 5 and 8) that occur in the original decomposition of our nourishment, and which we do not examine further here.

Our nourishments are also alongshore periodic. Such an interpretation clearly has relevance if we are considering a series of nourishments, as mentioned earlier. An isolated nourishment must, more correctly, be represented as a Fourier integral. While limiting again, the widely observed natural rhythmic bed features that evolve from non-periodic (natural) disturbances do indicate that there is evidence that a non-periodic disturbance expressed as a periodic one can lead to realistic predictions. We emphasise that we are looking at a succession of nourishments, as suggested by Koster (2006). Our successive nourishments cannot interact in our approach; different values of λ_1 are chosen to reflect nourishments that are further or closer apart and are motivated by typical length scales used in the field. We cannot give a criterion to distinguish possible interacting and non-interacting nourishments. It seems highly unlikely to us that our 6 km or 1.5 km spaced nourishments will interact significantly with each other before nonlinear effects and cross-shore processes make the linear analysis questionable. Remember that we consider too only normal incidence. Natural bed-forms (crescentic bars) can migrate approximately 20 m per day, but usually only in the presence of an alongshore current. Even allowing for this happening every day our decay over 50 days in Fig. 11 (to, note, negligible amplitudes at the original location) would correspond to a migration of 1 km for the 6 km spaced nourishment (now near the shore). For the 1.5 km nourishment a similar decay occurs over just 5 days. For our shorter scale nourishments their proximity is, of course, nearer to each other, but the large decay rates mean that they will have little chance to interact.

Furthermore, our doubly Gaussian nourishments show that this approach is physically plausible, because our nourishments are very widely spaced (isolated) and can physically be expected to behave in such a way.

All these restrictions must be borne in mind in interpretation. A fully nonlinear method will alleviate some of them. However, a realistic nonlinear evolution should start from a nourishment on a fully developed beach, to take into account the morphodynamic instabilities on a plane beach. It is also worth remembering that the present approach is massively less computationally expensive than traditional numerical modelling.

7. Conclusions

A method has been presented for representing shoreface nourishments in terms of natural modes of a morphodynamical system on an equilibrium beach, and therefore interpreting nourishments as perturbations of the natural system. Plane beaches are shown primarily to have a morphodynamic modal structure consisting of more decaying than growing modes, the decay rates of which depend on the forcing. Steeper beaches have faster decay rates. This expansion generally works well in terms of accurately representing the nourishments, although extremely long scale nourishments (more than 10 km) may not be expressible, and there are limitations on the positioning of the nourishments. The initial amplitudes of shorter scale nourishments also typically comprise more growing modes than long scale nourishments. All realistic scale nourishments are essentially diffusive (decaying), with longer scale nourishments migrating onshore as they decay. Longer scale nourishments decay much more slowly than shorter scale nourishments (amplitude decay to a third of the original height in about 50 days for computational time in our example, which is for energetic forcing conditions). All of this makes them more effective nourishments than those of shorter scale. This decay should be interpreted in terms of the amount of real time that the nourishment experiences these conditions, so that their real decay times are likely to be substantially longer. The approach has substantial limitations, but as a method for predicting the behaviour of nourishments it has relevance. Furthermore, it opens up the possibilities of nonlinear projection techniques to study nourishment behaviour.

Acknowledgements

S.M. van Leeuwen gratefully acknowledges the support of the UK Engineering and Physical Sciences Research Council (EPSRC) under grant GR/S19172/01. Partial funding by the Ministerio de Ciencia y Tecnologia of Spain through the PUDEM project under contract REN2003-06637-C02-01/MAR and through the "Ramón y Cajal" contract of D. Calvete is also gratefully acknowledged. Furthermore, S.M. van Leeuwen would like to thank the HPC-Europa Transnational Access programme under grant HPC04T35NT. This paper does not include results obtained from the HPC computing facilities but the research visit made to the HPC centre in Barcelona contributed significantly to the work presented here.

References

Calvete, D., De Swart, H., 2003. A nonlinear model study on the long-term behaviour of shoreface-connected sand ridges. J. Geophys. Res. C 108 (C5). 3169. doi:10.1029/2001JC001091.

Calvete, D., Dodd, N., Falqués, A., van Leeuwen, S.M., 2005. Morphological development of rip channels at normal and near normal incidence. J. Geophys. Res. C 110 (C10), C10007. doi:10.1029/2004JC002803.

Damgaard, J., Dodd, N., Hall, L., Chesher, T., 2002. Morphodynamic modelling of rip channel growth. Coast. Eng. 45, 199–221.

De Swart, H.E., Calvete, D., 2003. Non-linear response of shoreface-connected sand ridges to interventions. Ocean Dyn. 53, 270–277. doi:10.1007/s10236-003-0044-9.

Deigaard, R., Drønen, N., Fredsøe, J., Hjelmager Jensen, J., Jørgensen, M.P., 1999. A morphological stability analysis for a long straight barred coast. Coast. Eng. 36, 171–195 PII:S0378-3839(99)00005-8.

Dodd, N., Blondeaux, P., Calvete, D., De Swart, H., Falqués, A., Hulscher, S.J.M.H., Różyński, G., Vittori, G., 2003. Understanding coastal morphodynamics using stability methods. J. Coast. Res. 19 (4), 849–865.

Grunnet, N.M., Ruessink, B.G., 2005. Morphodynamic response of nearshore bars to a shoreface nourishment. Coast. Eng. 52, 119–137. doi:10.1016/j.coastaleng.2004.09.006.

Grunnet, N.M., Walstra, D.R., Ruessink, B.G., 2004. Process-based modelling of a shoreface nourishment. Coast. Eng. 51, 581–607. doi:10.1016/j.coastaleng.2004.07.016.

Hamm, L., Capobianco, M., Dette, H.H., Lechuga, A., Spanhoff, R., Stive, M.J.F., 2002. A summary of European experience with shore nourishment. Coast. Eng. 47, 237–264.

Hanson, H., Brampton, A.H., Capobianco, M., Dette, H.H., Hamm, L., Laustrup, C., Lechuga, A., Spanhoff, R., 2002. Beach nourishment projects, practices, and objectives—a European overview. Coast. Eng. 47, 81–111.

Hudson, J., Damgaard, J.S., Dodd, N., Cooper, A.J., Chesher, T.J., 2005. Approaches to 1d morphodynamical modelling in coastal engineering. Coast. Eng. 52 (8), 691–707.

Johnson, H.K., Appendini, C.M., Soldati, M., Elfrink, B., Sørenson, P., 2001. Numerical modelling of morphological changes due to shoreface nourishment. Coast. Dyn. 878–887.

Klein, M.D., 2005. Modelling rhythmic morphology in the surf zone. Ph.D. thesis, Delft University of Technology, Faculty of Civil Engineering, www.library.tudelft.nl/ws/a/resources_guide/tudelftpublicaties/zoeken/metadata/index.htm?docname=027961.

Koster, L., april 2006. Humplike nourishing of the shoreface. Master's thesis, Technical University Delft, Faculty of Civil Engineering, www.citg.tudelft.nl/live/binaries/4de0d195-5207-4e67-84bb-455c5403ae47/doc/2006Koster.pdf, (WL/Delft Hydraulics Tech. Report Z3873/Z3912).

Mei, C.C., 1989. The Applied Dynamics of Ocean Surface Waves. World Scientific, Singapore.

Reniers, A.J.H.M., Roelvink, J.A., Thornton, E.B., 2004. Morphodynamic modeling of an embayed beach under wave group forcing. J. Geophys. Res. C 109, C01030.

Roelvink, D., Reniers, A., Walstra, D.R., van Ormondt, M., 2005. Shoreface nourishments: humps or bars? Book of abstracts, Coastal Dynamics, Laboratori d'Enginyeria Maritima, UPC, pp. 316–317.

Roos, P.C., Blondeaux, P., Hulscher, S.J.M.H., Vittori, G., 2005. Linear evolution of sandwave packets. J. Geophys. Res. 110, F04S14. doi:10.1029/2004JF000196.

Soulsby, R., 1997. Dynamics of Marine Sands. Thomas Telford Publications, London.

Thornton, B., Guza, R.T., 1983. Transformation of wave height distribution. J. Geophys. Res. C 88 (10), 5925–5938.

van Duin, M.J.P., Wiersma, N.R., Walstra, D.J.R., van Rijn, L.C., Stive, M.J.F., 2004. Nourishing the shoreface: observations and hindcasting of the Egmond case, The Netherlands. Coast. Eng. 51, 813–837. doi:10.1016/j.coastaleng.2004.07.011.

van Enckevort, I.M.J., Ruessink, B.G., Coco, G., Suzuki, K., Turner, I.L., Plant, N.G., Holman, R.A., 2004. Observations of nearshore crescentic sandbars. J. Geophys. Res. C 109, C06028. doi:10.1029/2003JC002214.

Van Leeuwen, S.M., Dodd, N., Calvete, D., Falqués, A., 2006. Physics of nearshore bed pattern formation under regular and random waves. J. Geophys. Res. C 111 (F01023). doi:10.1029/2005JF000360.